Gallium nitride quantum dots in a nitrogen-bonded silica gel matrix

Gallium nitride quantum dots in a nitrogen-bonded silica gel matrix

Godhuli Sinha[1]**, Subhendu K Panda**[1]**, Pratima Mishra**[2]**,
Dibyendu Ganguli**[1] **and Subhadra Chaudhuri**[1,3]

[1] Department of Materials Science, Indian Association for the Cultivation of Science, Jadavpur, Kolkata 700 032, India
[2] Advanced Materials Technology Department, Regional Research Laboratory, Bhubaneswar 760 013, India

E-mail: mssc2@iacs.res.in (S Chaudhuri)

Abstract

GaN:SiO$_2$ nanocomposites were successfully synthesized by a two-step process. Firstly, an intermediate xerogel was obtained by the sol–gel method and, in the second step, annealing the powdered samples at 900 °C for 5 h in flowing NH$_3$ atmosphere produced the nanocomposites. X-ray diffraction and high-resolution transmission electron microscopic studies confirmed that the confined GaN nanoparticles (2–12 nm) were crystallized as a mixture of hexagonal and cubic phases. The optical band gap was observed to be enhanced slightly (3.69 eV) from the bulk value (3.39 eV) for the sample with the lowest molar ratio of GaN (10:90) in the nanocomposites. Fourier transform infrared spectroscopic studies indicated the formation of Ga–N bond along with probable signatures of Si–O, Si–N and Si–N–O bonds. The nanocomposites showed photoluminescence peaks at 370 and 571 nm as a result of excitation at 310 nm. Raman study of the samples shows peaks corresponding to the hexagonal and cubic phases of GaN.

1. Introduction

Efficient production of light-emitting crystalline nanoparticles is regarded as fascinating to materials scientists as, on decreasing the particle size, some distinctive properties are expected from nanostructures compared to the bulk materials [1–5]. Theoretical and experimental studies on materials of nanometer size indicate that the optical properties of these materials depend highly on their sizes, especially when they are comparable to the corresponding excitonic Bohr radius.

[3] Author to whom any correspondence should be addressed.

Technologically, it is very important to fabricate isolated nanoparticles [1–5]. However, nanoparticles can agglomerate easily due to their high surface energy. Therefore, it is difficult to obtain an isolated nanoparticle to study its individual properties. To avoid this, various modes of surface passivation have been considered, such as coating by protective organic molecules [6] or confinement in inorganic matrices [7–11]. Many research groups observed an enhancement of the photoluminescence (PL) properties when a material with a narrower band gap is dispersed in a wider band gap material [12, 13].

Gallium nitride, a III–V semiconductor material, is a promising candidate for applications in blue-to-UV light-emitting diodes, high-temperature/pressure device, laser diodes and optical modulator heterostructure field-effect transistors etc, due to its wide band gap, large excitation energy and large binding energy [14–18]. Previously, preparations of GaN nanostructures were handled by various physical techniques like pyrolysis [2], thermal chemical vapour synthesis [19], flame synthesis [20], and plasma synthesis [18]. However, the low reactivity of gallium metal with nitrogen, the low decomposition temperature of gallium nitride, and nitrogen stoichiometry issues make the process very difficult [21]. At ambient pressure, gallium nitride crystallizes with a hexagonal structure with a lattice constant $a = 3.19$ Å and $c/a = 1.627$ [22]. Xia *et al* [23] observed a pressure-induced first-order phase transition from hexagonal to cubic structure at a pressure of 37 GPa. Jegier *et al* [24] reported the formation of phase pure cubic GaN to be temperature-dependent and the formation of a mixture of hexagonal and cubic phase at a temperature of 350 °C under autogenic pressure. One of the most cost-effective methods for the synthesis of isolated GaN nanoparticles is to disperse them in a suitable matrix, for which silica has been chosen by several groups for the encapsulation of high-quality GaN nanoparticles [1, 4, 11].

In the present case, we have synthesized isolated GaN nanoparticles embedded in a silica matrix by the sol–gel method with particle sizes varying between 2 and 12 nm. Although the synthesis was carried out at ambient pressure, cubic GaN was found to accompany the hexagonal phase. The optical and microstructural properties of such embedded gallium nitride particles are characterized.

2. Experimental details

GaN nanoparticles in a silica matrix were prepared through two steps. First, a sol–gel method was adopted, which allowed us to synthesize an intermediate gel product with different molar ratios of gallium metal and silica (10:90, 20:80 and 30:70), respectively. At first, gallium metal (Aldrich, USA, 99.99%) was dissolved in a calculated amount of concentrated nitric acid. In the next step, a calculated amount of tetraethyl orthosilicate (TEOS, Merck Schuchardt) was dissolved in an ethanol–water mixture. Then, a few drops of 0.1 N HCl were added to it as a catalyst under rigorous stirring to form a sol. After 1 h of stirring, the gallium solution was slowly added to it. The pH value was observed to be about 1 in this case. After stirring for another 1 h, a clear solution was obtained, which was heated at about 70 °C for 3.5 h to enhance the hydrolysis and condensation processes. The clear gel obtained in this process was dried at 200 °C for 4 h. The xerogels thus obtained were placed in a horizontal furnace in an alumina boat and annealed at 900 °C for 5 h under a flowing (30 ml min^{-1}) NH$_3$ atmosphere and slowly cooled down to room temperature. It was observed that all the nanocomposite samples were of yellow colour. In this paper we have designated the samples with molar ratios 10:90, 20:80 and 30:70 as S1, S2 and S3, respectively.

The crystalline phases of the nanocomposite samples were determined by x-ray power diffractometer (XRD, Seifert 3000P) with Cu Kα radiation ($\lambda = 1.54178$ Å). The morphology and microstructural properties of the samples were obtained using a high-
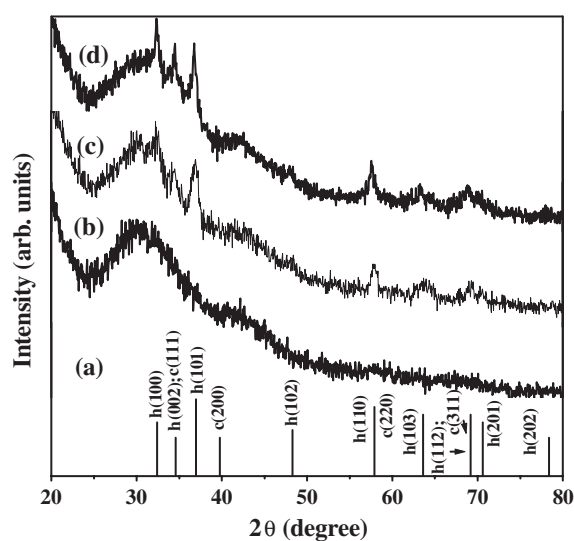
Figure 1. (a) Standard x-ray diffraction pattern of hexagonal and cubic phases of GaN. (b)–(d) XRD patterns of sample S1 (b), S2 (c) and S3 (d), respectively (annealed at 900 °C under a flowing NH_3 atmosphere (30 ml min^{-1})). All the patterns of the samples indicate a random arrangement of hexagonal and cubic phases.

resolution transmission electron microscope (HRTEM, JEOL 2010). For TEM studies, samples were ultrasonically dispersed in 2-propanol and a drop of the sample was placed on a carbon-coated copper grid. Fourier transform infrared (FTIR) studies were carried out using a MAGNA-IR 750 spectrometer. Optical transmittance spectra of the samples were recorded with an ultraviolet–visible–near-infrared (UV–vis–NIR) spectrophotometer (Hitachi, U-3410). Raman spectra were acquired with a Renishaw inVia Raman spectrometer, which is amenable to obtain data in the micro range. The excitation source was a 514 nm argon ion laser with 100% power. The resolution of all the spectra was within ± 2 cm^{-1}. All the spectra were analyzed using the software supplied by Renishaw and background corrections were made when needed. Room-temperature photoluminescence (PL) measurements were carried out using a fluorescence spectrophotometer (Hitachi FL 2500).

3. Results and discussion

3.1. XRD studies

Figure 1 shows the XRD patterns of the nanocomposite samples with different molar ratios. The patterns reveal that GaN nanoparticles are crystallized as a mixture of both hexagonal and cubic phases after nitridation for 5 h at 900 °C in a flowing NH_3 atmosphere (30 ml min^{-1}). The absence of XRD peaks of gallium oxide indicates the complete transformation of the gallium metal into GaN. XRD patterns of the samples also indicate that the crystallinity of the S3 is greater than that of S2 and S1, i.e. the crystallinity of the samples increases with increasing molar percentage of gallium nitride in the composite. The (100), (002), (101), (110) and (112) peaks of the hexagonal phase of GaN are clearly observed in the XRD patterns of the samples (figures 1(b)–(d)). The existence of the (103) peak of the hexagonal structure becomes less discernible in the pattern for S1 compared to those for S2 and S3. However, the peak at $2\theta = 39.76$, representing the (200) plane of the cubic system [24], is distinguishable only
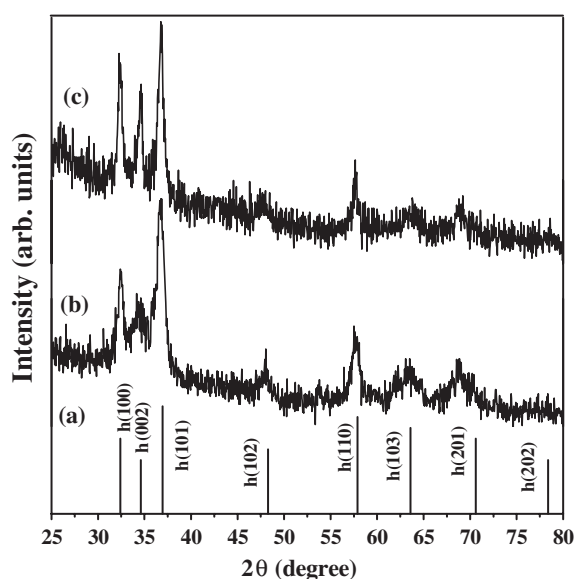
Figure 2. XRD patterns of sample (a) S2 and (b) S3 after nitridation at 1000 °C for 5 h (90 ml min^{-1}). With increasing nitridation temperature, traces of cubic phase have gone astray.

for samples S2 and S3 and slightly shifted towards a higher 2θ value for sample S1. Broad peaks in the XRD patterns of the samples indicate that the sizes of the particles were very small and that the patterns agree well with previous reports [5, 10, 11]. These observations are in obvious contrast to those reported by Iskandar *et al* [25], who prepared unrestricted and agglomerated hexagonal gallium nitride nanoparticles (20–50 nm), showing sharp XRD peaks under similar annealing condition. It is well known that GaN particles in general crystallize in the cubic system under high pressure [23], and transform to a hexagonal system on decreasing the pressure. On the other hand, it has been observed that crystallization of a mixture of hexagonal and cubic GaN takes place under autogenic pressure and at a temperature of approximately 200 °C [24, 26, 27]. From the phase diagram for GaN [28], it is evident that, at a temperature >1200 °C, it is necessary to apply a pressure >1.0 GPa in order to obtain the thermodynamically stable product. In the present case, GaN nanoparticles are confined within the silica matrix, which presumably has a consequence in the formation of a large numbers of stacking faults. These stacking faults result in the crystallization of GaN nanoparticles in a random arrangement of hexagonal and cubic systems without any additional pressure [29]. Crystallization of cubic GaN nanoparticles in addition to hexagonal GaN under ambient pressure, as observed in the present work, has apparently not been reported before. Figure 2 shows the XRD patterns of the nanocomposite samples obtained at a nitridation temperature of 1000 °C and in a flowing NH$_3$ atmosphere with a flow rate of 90 ml min^{-1}. It was observed that all are crystallized in the pure hexagonal phase. This indicates that, with increasing temperature, there is an increase in the size of the particles, which may reduce the number of stacking faults, and finally the particles are crystallized in hexagonal symmetry.

3.2. Microstructural studies

Figures 3(a)–(f) show TEM images of GaN:SiO$_2$ nanocomposites. The TEM image of sample S1 (figure 3(a)) shows isolated spherical GaN nanoparticles embedded in the SiO$_2$ matrix.
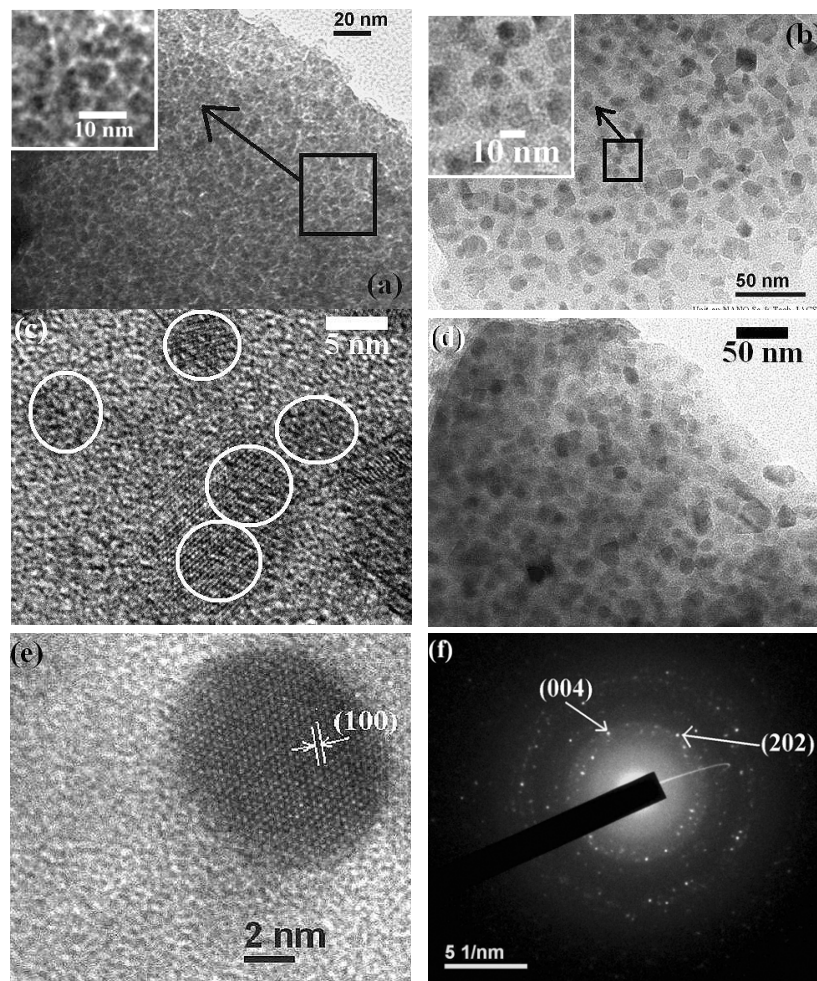
4

Figure 3. (a) and (b) TEM images of sample S1 and S2, respectively; the inset shows a closer view of the marked part in the corresponding figures; (c) HRTEM image of sample S2. (d) TEM image of sample S3. (e) and (f) HRTEM image of a single particle and SAED pattern of sample S3, respectively.

However, in some of the portions, the particles coalesce together to form bigger particles. The size of the particles varies from 2 to 5 nm. The inset of figure 3(a) shows a few GaN nanoparticles with a size of 3 nm surrounded by silica matrix. Figure 3(b) reveals that, in the sample S2, some of the particles are distorted cubic and other particles are spherical in shape, with one side slightly elongated. In some portions, the particles coalesce together to form larger particles, though the individual particles are discernible enough for size measurement as against freely formed GaN particles [25]. The inset of figure 3(b) shows a clear view of some gallium nitride particles embedded in silica matrix. The particle size of this gallium nitride composite varies from 3 to 8 nm. The HRTEM image (figure 3(c)) of sample S2 indicates the formation of the (102) plane of a hexagonal phase of GaN. Also, in the case of sample S3, distorted cubic and spherical GaN nanoparticles dispersed in silica matrix (figure 3(d)) are observed, where the size of the particles varies in a range between 8 and 12 nm. The HRTEM
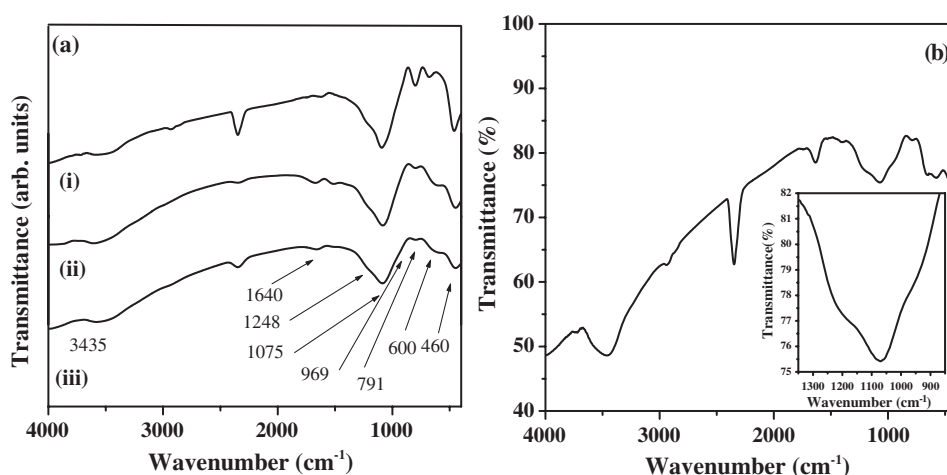
Figure 4. (a) Comparative studies of FTIR spectra of sample (i) S1, (ii) S2 and (iii) S3. (b) FTIR spectrum of the composite with a molar ratio of 30:70 with nitridation at 900 °C/5 h in a NH$_3$ atmosphere at a flow rate 90 ml min^{-1}.

image of sample S3 (figure 3(e)) shows an isolated GaN particle in silica matrix. The lattice spacing is calculated to be 0.28 nm, which corresponds to the (100) plane of hexagonal GaN. The selected-area electron diffraction (SAED) pattern of sample S3 (figure 3(f)) shows the ring patterns, indicating the polycrystalline nature of GaN nanoparticles. The dots on the rings correspond to (004) and (102) planes of the hexagonal phase.

3.3. FTIR spectroscopy

FTIR spectroscopy was performed in order to evaluate formations and distortions of chemical bonds. Figure 4(a) shows a comparative study of FTIR spectra of samples S1, S2 and S3. A hump at ∼3435 cm^{-1} can be observed in the spectra of all the samples, which may be assigned to the stretching of strongly hydrogen-bonded –OH groups [30–32]. The bond is shifted towards higher frequency with an increase in the molar ratio of GaN in the composite. The appearance of a weak peak ∼1640 cm^{-1} may be due to the presence of 'unsaturated' Ga^{3+} ions on the surface [33]. Thus it can be concluded that the amount of gallium that can be incorporated in the silica gel matrix is very small. The presence of the referred band is weaker in the spectrum of the samples with a smaller molar ratio of GaN in the nanocomposite, which is in good agreement with that observed by Areàn *et al* [33]. In each spectrum, a broad peak in the range from 1324 to 864 cm^{-1} can be observed. A shoulder near 1248 cm^{-1} appears due to stretching of Si–O–Si bond. The peak with the highest intensity at 1081 cm^{-1} can be assigned to asymmetric stretching. Diniz *et al* [34] assigned the peak near 1075 cm^{-1} to stretching of Si–O bonds. The features of the absorption spectra of samples S2 and S3 in the region around 969–847 cm^{-1} are attributed to the formation of the Si–N–O bond in silicon oxynitride [34, 35] and the shoulder ∼951 cm^{-1} may represent a Si–N–Si bond [36, 37]. Brinker and Haaland [38] reported the presence of a Si–N bond at ∼970 cm^{-1}, which could be shifted depending upon the O/N atom ratio, but no such absorption peak appeared in the present spectrum. An absorption peak at ∼791 cm^{-1} appeared due to the bending mode of the Si–O–Si bond [39]. A broad peak is observed at ∼600 cm^{-1}, which may be due to the formation of the Ga–N bond [40]. The absorption peak appearing at ∼460 cm^{-1} can be assigned to the wagging
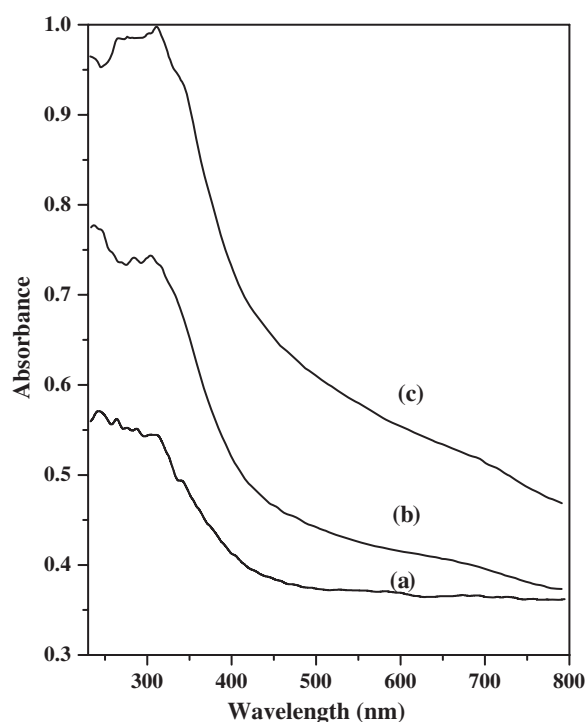
Figure 5. UV–visible absorbance versus wavelength traces of sample (a) S1, (b) S2 and (c) S3.

mode of Si–N bonds [34]. On annealing sample S3 at 900 °C for 5 h under a high NH_3 flow rate (90 ml min^{-1}), a slightly different pattern can be observed, as shown in figure 4(b). The shoulder at ∼951 cm^{-1} becomes more prominent in this case (see the inset of figure 4(b)), indicating the formation of more Si–N–Si bonds. Therefore from these observations it can be concluded that, during nitridation of gallium precursor in silica matrix, a little amount of NH_3 diffused in the silica and resulted in the formation of the Si–O, Si–N, Si–N–O bonds.

3.4. Optical studies

Optical characterization of the nanocomposite samples was carried out by UV–visible spectroscopy at room temperature after dispersing the sample ultrasonically in water. Figure 5 (curves (a)–(c)) shows a comparative study of absorbance versus wavelength spectra of the $GaN:SiO_2$ nanocomposites. These spectra show that the characteristic absorption edge shifts towards a longer wavelength on increasing the molar percentage of GaN in the nanocomposite. The optical band gap value (E_g), obtained by taking the derivative of the absorbance spectra, is the highest (3.69 eV) for sample S1, and the values for samples S2 and S3 are calculated to be 3.50 eV and 3.39 eV, respectively. The Bohr radius of gallium nitride has been estimated to be 11 nm [41]. Therefore a considerable blue shift in the absorption spectra indicates the quantum confinement effect on decreasing the size of GaN particles in the nanocomposites.

3.5. Raman spectroscopy

Hexagonal GaN belongs to the Pb_3mc (C_{6v}^4) space group having four electrons in the unit cell. At $k = 0$, group theory predicts $\Gamma_{12} = 2A_1 + 2B_1 + 2E_1 + 2E_2$, in which one A_1, one E_1
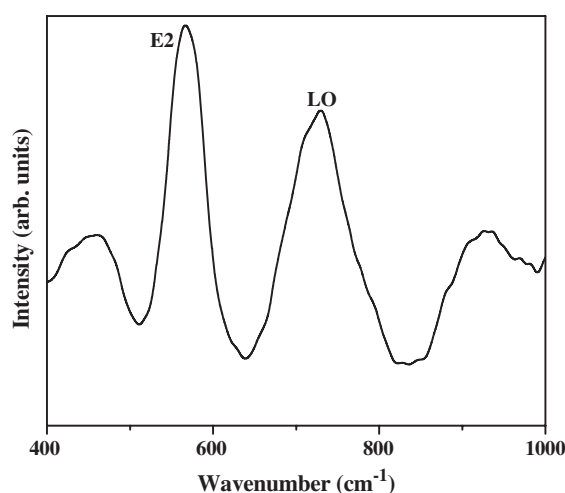
Figure 6. Raman spectrum of GaN:SiO$_2$ composite with a molar ratio of 30:70 (S3).

and two E$_2$ are Raman active [42]. Figure 6 is a representative Raman spectrum of sample S3, which shows two broad peaks at ∼567 and 729 cm^{-1}. Of these, 567 cm^{-1} is a well-known mode of E2 symmetry of hexagonal gallium nitride, and 729 cm^{-1} can be assigned for the LO phonon A1 symmetry of hexagonal gallium nitride [43, 44]. Cubic gallium nitride shows a very similar Raman spectrum to the hexagonal gallium nitride (cubic TO phonon at 555 cm^{-1} and LO phonon at 740 cm^{-1}) [43, 44]. The peaks indicating that hexagonal and cubic symmetry may merge together and lead to the broadening of the peaks. There is a possibility of fluctuation of wavevector associated with the size distribution, which may induce the broadening of Raman peaks. In the present case, no peaks due to the Si–N bond at 620 cm^{-1} (TO + TA) and 920 cm^{-1} (2TO) [45] are observed.

3.6. Photoluminescence studies

Photoluminescence spectra of samples S1, S2 and S3 were recorded at room temperature with excitation at 310 nm (figure 7). All the samples exhibit near-band-edge emission at 370 nm and yellow luminescence at 570 nm. The spectra shown in figure 7 indicate that the intensity of near-band-edge emission is highest for sample S3 and goes on decreasing for samples S2 and S1. This may be due to the more highly crystalline nature of sample S3 than sample S2 and S1. The reverse trend can be observed for yellow luminescence. The intensity of yellow luminescence increases with decreasing molar ratio of GaN in the nanocomposites i.e. the intensity is the highest for sample S1 and goes on decreasing for samples S2 and S3. Dominant optically active defects in general originate from the yellow luminescence in GaN [46]. Neugebauer and Van de Walle [47] proposed that a native defect, namely the Ga defect, is the microstructural origin of the yellow luminescence. A smaller particle size for sample S1 (2–5 nm) may induce the formation of a large number of Ga defects than samples S2 (3–8 nm) and S3 (8–12 nm). This fact probably results in the tailoring intensity of yellow luminescence.

4. Conclusion

GaN nanoparticles (2–12 nm), well dispersed in silica matrix, were prepared using the sol–gel method with different molar ratios (10:90, 20:80 and 30:70). XRD patterns and HRTEM studies
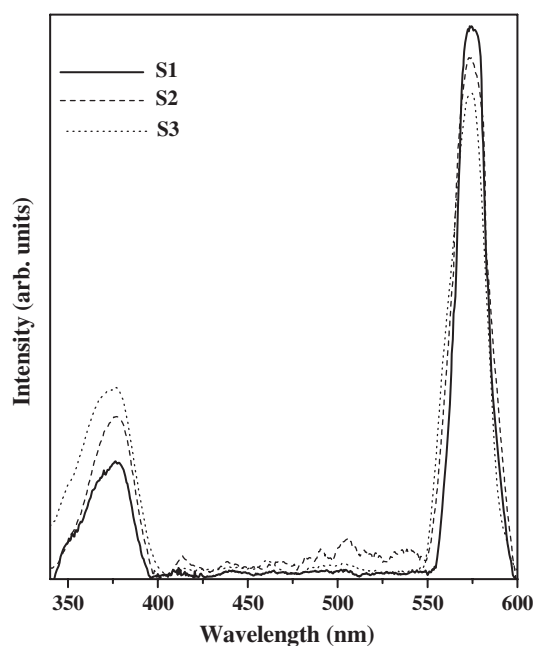
Figure 7. Photoluminescence spectra of the sample (i) S1 (solid line), (b) S2 (dash line) and (c) S3 (dotted line) with excitation at 310 nm.

confirmed that the GaN nanoparticles in the silica matrix were crystallized in an assemblage with a random arrangement of the hexagonal and cubic structures. At ambient pressure, the hexagonal structure is the most stable form of GaN. However, the growth of c-GaN is known to be difficult, because the cubic phase is a metastable polytype. In the present case, the gallium nitride particles were confined within a silica matrix, which probably caused the formation of stacking faults and resulted in the random arrangements of the hexagonal and cubic phases. By increasing the nitridation temperature and the flow rate of NH_3 gas, GaN nanoparticles embedded in silica matrix were observed to be crystallized in the pure hexagonal phase. The optical band gap of the $GaN:SiO_2$ nanocomposites increased with decreasing molar percentage of GaN in the composites. FTIR studies confirmed a slight diffusion of nitrogen into the matrix at the time of nitridation of the samples and indicated the formation of Si–O, Si–N–O and Si–N bonds. Considerably broad peaks in Raman spectra confirmed the nanocrystallinity, and indicate that the gallium nitride particles possess both hexagonal and cubic symmetry. GaN particles exhibit luminescence properties with tailorable intensity.

Acknowledgments

References

[1] Li L and Shi J L 2006 *Nanotechnology* **17** 344
[2] Shimada M, Azuma Y, Okuyama K, Hayashi Y and Tanabi E 2006 *Japan. J. Appl. Phys.* **45** 328

[3] Kayanuma Y 1988 *Phys. Rev.* B **38** 9797
[4] Zhao X G, Shi J, Hu L B, Zhang L X and Hua Z L 2003 *J. Mater. Chem.* **13** 399
[5] Murali A K, Leppert V J and Risbud S H 2000 *Mater. Sci. Eng.* B **76** 206
[6] Lee S W and Choi C S 2007 *Micron* **38** 58
[7] Sinha G, Ganguli D and Chaudhuri S 2006 *J. Phys.: Condens. Matter* **18** 11167
[8] Gorai S and Chaudhuri S 2006 *Mater. Sci. Eng.* B **126** 97
[9] Chakrabarti S, Ganguli D and Chaudhuri S 2003 *J. Phys. D: Appl. Phys.* **36** 146
[10] Que H, Cao C, Wang D and Zhu H 2006 *Mater. Chem. Phys.* **96** 296
[11] Yang Y, Tran C, Leppert V and Risbud S H 2000 *Mater. Lett.* **43** 243
[12] Peng X G, Schlamp M C and Kadavanich A V 1997 *J. Am. Chem. Soc.* **119** 7019
[13] Dabbousi B O, Rodriguez-Viejo J, Miculec F V, Heine J R, Mattoussi H, Ober R, Jensen K F and
     Bawendi M G 1997 *J. Phys. Chem.* B **101** 9463
[14] Wang L, Liu X, Zan Y, Wang J, Wang D, Lu D E and Wang Z 1998 *Appl. Phys. Lett.* **72** 109
[15] Lie T, Moustakas T D, Graham R J, He Y and Berkowitz J 1992 *J. Appl. Phys.* **71** 4933
[16] Ponce F A, Dupuis R D, Nakamura S and Edmond J A 1995 *Proc. Materials Research Society Mtg Boston on
     Gallium Nitride and Related Materials: The 1st Int. Symp. on Gallium Nitride and Related Materials*
[17] Strite S, Lin M E and Morkoc H 1993 *Thin Solid Films* **213** 197
[18] Nakamura S, Mukuai T and Senoh M 1994 *Appl. Phys. Lett.* **64** 1687
[19] Janik J F and Wells R L 1996 *Chem. Mater.* **8** 2708
[20] Azuma Y, Shimada M and Okuyama K 2004 *Chem. Vapor Depos.* **10** 11
[21] Tani T, Mädler L and Pratsinis S E 2004 *J. Nanopart. Res.* **4** 337
[22] Shultz H and Thiemann K H 1977 *Solid State Commun.* **23** 815
[23] Xia H, Xia Q and Ruoff A L 1993 *Phys. Rev.* B **47** 12925
[24] Jegier J A, McKernan S, Purdy A P and Gladfelter W L 2000 *Chem. Mater.* **12** 1003
[25] Iskandar F, Ogi T and Okuyama K 2006 *Mater. Lett.* **60** 73
[26] Purdy A P 1999 *Chem. Mater.* **11** 1648
[27] Xia Y, Qian Y, Wang W, Zhang S and Zhang Y 1996 *Science* **27** 1926
[28] Karpinski J, Jun J and Porowski S 1984 *J. Cryst. Growth* **66** 1
[29] Hwang J W, Campbell J P, Kozubowski J, Hanson S A, Evans J F and Glafelter W L 1995 *Chem. Mater.* **7** 517
[30] Brinker C J and Scherer G W 1990 *Sol Gel Science* (San Diego, CA: Academic) chapter 3
[31] Fidalgo A, Nunes T G and Ilharco L M 2000 *J. Sol–Gel Sci. Technol.* **19** 403
[32] Innocenzi P, Falcaro P, Grosso D and Babonneau F 2003 *J. Phys. Chem.* B **107** 711
[33] Areàn C O, Delgado M R, Montouillout V, Lavalley J C, Fernandez C, Pascual J J C and Parra J B 2004 *Micropor.
     Mesopor. Mater.* **67** 259
[34] Diniz J A, Tatsch P J and Pudenzi M A A 1996 *Appl. Phys. Lett.* **69** 2214
[35] Lange P, Bernt H, Hartmannsgruber E and Naumann F 1994 *J. Electrochem. Soc.* **141** 259
[36] Socrates G 2001 *Infrared and Raman Characteristic Group Frequencies: Tables and Charts* (New York: Wiley)
[37] Chen Z, Prasad K, Li C Y, Su S S, Gui D, Lu P W, He X and Balakumar S 2004 *Thin Solid Films* **462/463** 223
[38] Brinker C J and Haaland D M 1983 *J. Am. Ceram. Soc.* **66** 758
[39] Barbosa G N and Oliveira H P 2006 *J. Non-Cryst. Solids* **352** 3009
[40] Kisailus D, Choi J H and Lange F F 2003 *J. Cryst. Growth* **249** 106
[41] Yoon J W, Sasaki T, Roh C H, Shim S H, Shim K B and Koshizaki N 2005 *Thin Solid Films* **471** 273
[42] Siegle H, Kaczmarczyk G, Filippidis L, Litvinchuk A P, Hoffmann A and Thomsen C 1997 *Phys. Rev.* B **55** 7000
[43] Coffer J F, Zerda T W, Appel R, Wells R L and Janik J F 1999 *Chem. Mater.* **11** 20
[44] Siegle H, Eckey L, Hoffmann A, Thomsen C, Meyer B, Schikora D, Hankein M and Liscchka K 1995 *Solid State
     Commun.* **96** 943
[45] Xin Y, Huang Z X, Shi Y, Pu L, Zhang R and Zheng Y D 2005 *Physica* E **30** 41
[46] Reiger W, Dimitrove R, Brunner D, Rohrer E, Ambacher O and Stutzmann M 1996 *Phys. Rev.* B **54** 17596
[47] Neugebauer J and Van de Walle C G 1996 *Appl. Phys. Lett.* **69** 503